Journal of Minerals and Materials Characterization and Engineering, 2022, 10, 338-359
https://www.scirp.org/journal/jmmce
ISSN Online: 2327-4085
ISSN Print: 2327-4077

Characterization of Clay Materials and Performance Evaluation of Fired Clay Composites Made for Low-Cost Housing

Paulette Cathy Mengue[1*], Michel Mbessa[1], Rodrigue Cyriaque Kaze[2], Adeyemi Adesina[3], Chrispin Pettang[1]

[1]Department of Civil Engineering, National Advanced School of Engineering, University of Yaoundé I, Yaoundé, Cameroon
[2]Laboratory of Applied Inorganic Chemistry, Faculty of Science, University of Yaoundé I, Yaoundé, Cameroon
[3]Department of Civil and Environmental Engineering, University of Windsor, Windsor, Canada
Email: *mangapaulettecathy@gmail.com

How to cite this paper: Mengue, P.C., Mbessa, M., Kaze, R.C., Adesina, A. and Pettang, C. (2022) Characterization of Clay Materials and Performance Evaluation of Fired Clay Composites Made for Low-Cost Housing. *Journal of Minerals and Materials Characterization and Engineering*, **10**, 338-359.
https://doi.org/10.4236/jmmce.2022.104024

Received: April 22, 2022
Accepted: July 9, 2022
Published: July 12, 2022

Abstract

This study deals with the physico-chemical, mineralogical and geotechnical characterization of alluvial clays from Batchenga in Cameroon with a view to their use as building materials for housing. The alluvial clay (Arg.All) was collected in the locality of Batchenga at the village Natchigal (4˚20'40"N and 11˚37'40"E at 378 m altitude) and was fired between 900˚C and 1100˚C. Characterization was performed by XRD, XRF, DTA/DTG, and firing tests. XRD, XRF, DTA/DTG infrared analysis methods were performed on these clays. The linear shrinkage, mechanical strengths, water absorption, porosity and density were measured on the fired products. The results obtained show that the major oxides are for the Arg.Lat SiO_2 (72.13%), Al_2O_3 (14.1%), Fe_2O_3 (4.45%) and for the Arg.All: SiO_2 (48.91%), Al_2O_3 (23.79%), Fe_2O_3 (9.54%). The fired products based on alluvial clay, present the flexural strength of 4.45 MPa at 900˚C and 6.80 MPa at 1100˚C. As for those based on lateritic clay, the flexural strength is 0.53 and 0.76 MPa respectively at 900 and 1100˚C. The porosity is 33.69% at 900˚C and 22.93% at 1100˚C for the alluvial clay and 39.55% at 900˚C and 36.01% for the lateritic clay at 1100˚C. Water absorption is 18% to 11.16% for alluvial clay and 22.43% to 21.16% for lateritic clay at 900˚C and 1100˚C respectively. These results suggest that alluvial clay and its firing products have better physico-chemical, geotechnical and mechanical characteristics regardless of the firing temperature of the manufactured products. The addition of degreaser is recommended to improve the mechanical performance of lateritic clay.

Keywords

Clays, Fired Products, Firing Temperature, Physical and Mechanical Properties, Microstructure

1. Introduction

Since ancient times, clays have been used as a raw material of geological origin, particularly in the production of coarse or construction-grade ceramics. The archaeological objects such as the gigantic constructions ("tower of Babel"), the numerous statuettes and strange potteries testify the existence of this ancient ceramic [1]. Their very great sensitivity to water makes them not only difficult materials to handle but also the object of several scientific studies. The techniques related to their use are increasingly innovative, compaction to firing, or from compaction to stabilization with a diversity of all kinds of stabilizers [2] [3]. In addition, the cost of conventional building materials, ignorance of clay raw materials are all difficult factors that hinder the initiation of decent and low-cost housing construction in Cameroon. Cameroon's population being 28.2 million with an estimated population growth of 3.9% (MINDUH, 2018) leads to a deficit of adequate housing. To meet the housing needs of this growing population, there is a need to promote the use of alternative building materials that are locally available and cost-effective.

For the World Resources Institute, the development of clays has ripple effects on the national economies of countries and the increase in their consumption is corollary to the increase in populations in the world (WRI, 2007; UNDP, 2011). Their use is therefore an alternative to expensive imported materials and a source of foreign currency deficit. Their exploitation also promotes youth employability, scientific innovation and economic growth [4]. They are the main raw materials exploited in industrialized developed countries. As a result, they have been the subject of several studies each time improving their value in terms of cost, energy in production, mechanical strength and even aesthetics [5] [6] [7]. Most of the developing countries (DC) such as Cameroon, are striving and active in the research, discovery and exploration of new clay deposits for their characterization and development. In order to make the clay sector productive, Cameroon did not hesitate to create the Mission for the Promotion of Local Clay Materials (MIPROMALO) by decree 90/1553 of September 18, 1990. This structure is in charge of valorizing and popularizing the use of clay materials in the whole territory in order to reduce the costs of realization of national equipment. Since gold, there are many brick factories and other initiatives working in the production and promotion of ceramic products in Cameroon. However, the use of clay products has remained low and is little sought after by the public. One wonders whether this lack of interest in these clay products is due to the quality of the raw material or to the quality of their firing products. Ceramics are scientifically

recognized as durable building materials. According to previous studies, all regions of Cameroon have significant evidence of industrial clays of various origins: sedimentary, residual and alluvial [8]. The valorisation of clay materials is of increasing interest in Cameroon. Current areas of interest are geopolymers [3] [9] [10] [11], nanocomposite materials [12] and ceramics [5] [13]-[19]. The results obtained are varied and mixed on the quality of their cooking product. Indeed, the region of Batchenga locality in southern Cameroon located at the confluence of the Congo and Lake Chad basins is influenced by the variants of these two climates. As one moves away from Batchenga East (Akok) towards Batchenga North (Otibili/Nachtigal), the lush forest vegetation disappears and gradually reveals a shrubby savannah, hence the interest in studying the clays that are victims of such an influence located between two climatic zones in order to observe their specificity as construction materials. In the same way, the Batchenga clays will only be useful to the natives if reliable data are available.

Geographical and Geological Setting

The locality of Batchenga is located 60 km from the city of Yaoundé, in the southern plateau of Cameroon, more precisely in the Centre region, on the National Road N˚ 1 Yaoundé, Nanga-Ebogo. Its surface area is approximately 216 km^2. In geographical coordinates, it extends from latitude 4˚22' to 4˚32' North and longitude 11˚62' to 11˚72' East (**Figure 1**). The average rainfall is 1525.1 mm, 1988-2018 with an average annual temperature of 23.5˚C. This region is characterized by an equatorial Guinean climate and a dendritic drainage network along the Sanaga River. Batchenga is located in the middle of the so-called "African Surface I" of the early Tertiary. Work carried out in the Ntui sector shows that the region is a peneplain with a relatively low relief with an average altitude of 520 m [20]. The geomorphology of Batchenga can be subdivided into three morphological units. The zone with an altitude of less than 475 m represents an average of 8% and is made up of valley bottoms that are easily flooded. The zone of altitude between 475 - 535 m represents approximately 85%. This zone is characterized by low slope whose grounds are urbanizable. The zone of altitude above 535 m represents about 7% and is made up of slopes and hills that are very difficult to develop. According to Vallerie (1995), the shape of the area is made up of plains with very little marked talwegs. The lowering of the topography here is due to tectonic undulations. Geologically, Batchenga is in the Yaoundé Group according to the Petro structural classification [21], and is of Neoproterozoic age. The mineral paragenesis of the Yaoundé series is essentially composed of migmatites and quartz mica schists, potassium feldspars associated with plagioclases, biotites, garnets and secondarily sillimanite. The rocks encountered are granites, parallelepiped and orthodiped gneisses all migmatized and emplaced in an epicontinental paleoenvironment [22]. The bedrock consists of four main lithological groups including the migmatite and migmatitic gneiss group, the amphibolite group, the micaschist group and the micaceous quartzite

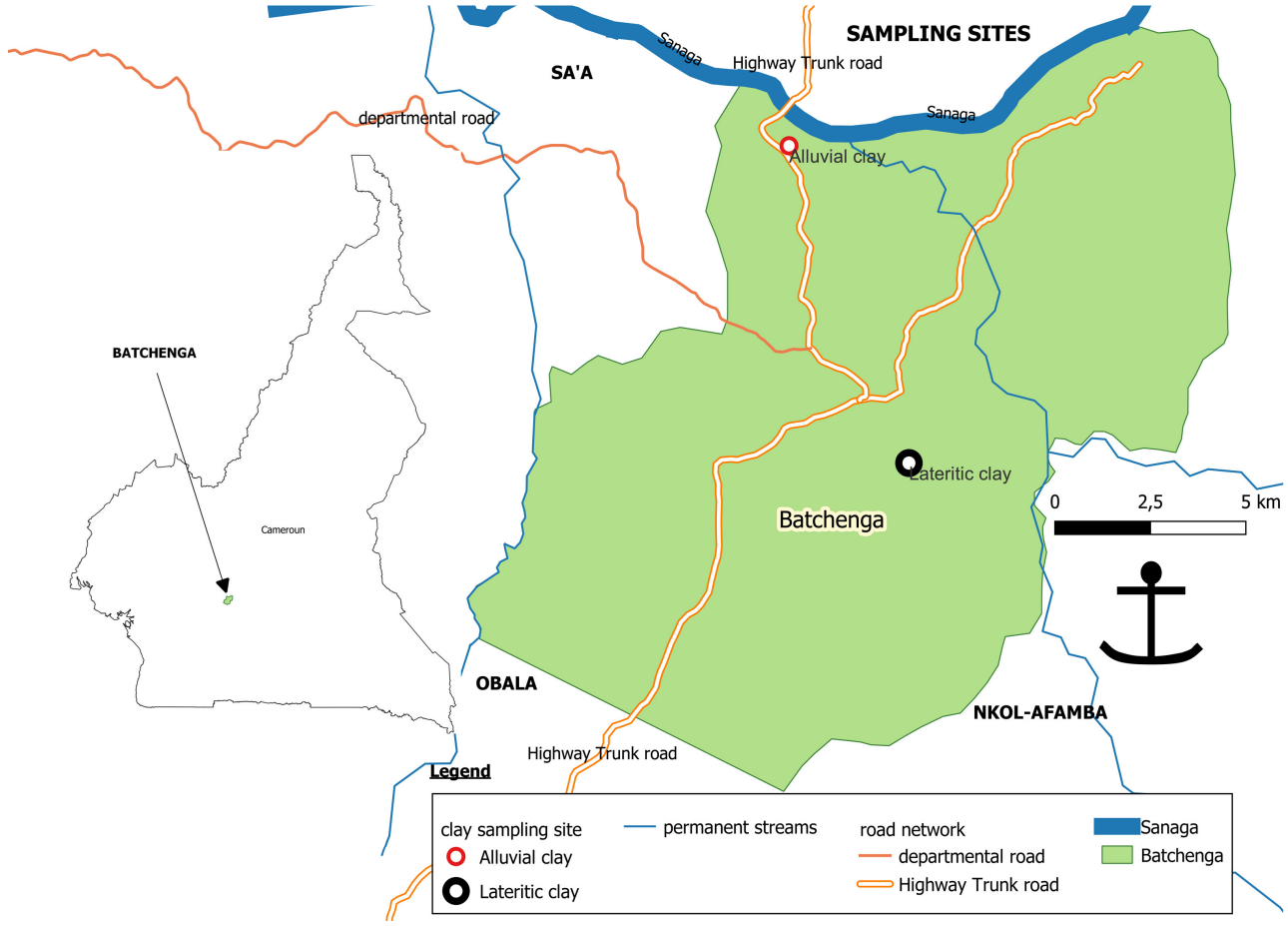

Figure 1. Source of clay samples.

group [20]. According to the geological sketch of the region, the Batchenga sector, which is located on the left bank of the Sanaga River, is mostly composed of migmatitic gneisses.

2. Materials and Methods

2.1. Samples and Sampling Techniques

Two clay samples were collected using a hand auger from different locations. One of the clay samples is alluvial clay (Arg.All) obtained from a section of the alluvial terrace near the Nachtigal stream located at coordinates of 4˚20'40"N and 11˚37'40"E, elevation of 378 m elevation and approximately 1.5 m depth from the surface. The second clay sample is lateritic clay (Arg.Lat) was also sourced locally in Cameroon and was collected about 2 km from the center of Batchenga. The location of the clay samples used in this study is indicated in Figure 1. Before sampling the clay samples, various identification tests such as visual, touch, odor test, hand washing test and "cigar" test were carried out.

2.2. Production of Clay Composites

Clay composites are made from the raw clay samples obtained and the influence

of firing temperatures evaluated. The clay composites were made by first mixing the humidified clay samples and packing the clay in a mould. A hydraulic pressure was used to apply a pressure of 10 MPa on the packed clay to ensure its well compacted in the moulds. After compaction, the filled moulds were subjected to firing in a muffle furnace with temperature ranging from 900˚C to 1100˚C at a rate of 5˚C/min for 3 hours. The firing procedures was carried out in a three-step cycles which entailed controlled increase in temperature, maintenance of temperature at desired value and cooling.

2.3. Test Methods

The colour of the clay samples was determined by using the Munsell soil colour chart on dry samples and cooked products. This colour determination was made by visual comparison with those of standard soils recorded in the Munsell colour map.

The mineral composition of the collected clay samples (*i.e.* Arg.all and Arg.Lat) was evaluated using x-ray diffraction methodology. The x-ray diffraction was performed with a Brucker D8-Advance diffraction apparatus (copper Kα1 radiance, λ = 1.541838 Å, V = 40 kV, I = 30 mA). Measurements were made in the 2θ range from 2˚ to 45˚ with a step size of 0.02˚ and a time per step of 2 s. Mineral identification on the diffractograms and a semi-quantitative mineralogical composition were processed using EVA software. The relative abundance of minerals was estimated from the heights of the main peaks.

The thermal analysis (*i.e.* DTA/TGA) of the samples was performed using a multidetector high-temperature calorimeter (Setaram 85) in a dry environment with a heating rate of 5˚C/min from room temperature to 1200˚C. For infrared analysis, samples of the clay materials and clay composites produced from the clay samples were finely ground to achieve a maximum particle size of 80 µm. During the test, an incident infrared beam is sent through the specimen that is to be analyzed and only wavelengths corresponding to an energy equal to the vibrational levels of the molecules in the samples were absorbed.

The chemical analysis of the samples was performed by emission spectrometry. The instrument used was a Bruker S4 Pioneer spectrometer. The sample was first crushed in an agate mortar. Then a mass of about 300 mg is taken and mixed with a mass of 900 mg of lithium metaborate ($LiBO_2$) in a Pt/Au crucible. The crucible containing the mixture is then heated for one hour at a temperature of 980˚C. The melted mixture is then dissolved in a 1.55 M nitric acid (HNO_3) solution placed in a polypropylene vessel and stirred at 20˚C for twelve hours. International standards BIR-1-0949, SDU-1-0295 and SDU-1-0296 as well as internal standards were used.

The particle size analysis was carried out by the sieve method for materials larger than 100 µm (NF P-18-560) and by sedimentometry (NF P 94 - 057) for those smaller than 100 µm. An electric agitator was used for the sieving method. Sedimentometry was based on the principle of Stoke's law of sedimentation of individual spherical particles falling freely at constant velocity under the influ-

ence of gravity. Atterberg limits were obtained by the Casagrande box method using ASTM D-422-63.

Prior to shaping the specimens, the Arg.All and Arg.Lat clays underwent drying, grinding, and sieving ≤ 315 μm. The Arg.All material was first dried at ambient atmosphere for one week before being oven dried. Then, both materials were oven dried at 105˚C temperature. The 315 μm sieve passings represent the fine fraction. The water content varies from 18% to 22% depending on the type of clay. The 4 × 4 × 16 cm and 2 × 4 × 8 cm specimens were made with a 10 KN hydraulic press and dried at room temperature for 7 days before being steamed at 105˚C for 24 hours to remove absorbed water before firing. The specimens formed from the clay materials are fired at 900˚C, 1000˚C, and 1100˚C for a period of 5 hours at a heating rate of 5˚C/min in a muffle furnace (Naberthem), Model 60/40. The clay composites obtained after firing are referred to as Arg.Lat900, Arg.Lat1000 and Arg.Lat1100 for the lateritic clay material and Arg.All900, Arg.All1000 and Arg.All1100 for the alluvial clay. 900, 1000 and 1100˚C represent the firing temperatures.

Firing shrinkage, water absorption and porosity were used to assess the durability performance of the clay composites. The firing shrinkage (L) was determined in accordance with ASTM C 531 (2000) by measuring L_O and L_T the lengths of the specimen before and after firing at temperature T. The firing shrinkage was obtained using Equation (1). The water absorption (WA) was determined as per ASTM C 20 (2000). The WA was expressed as a percentage of the ratio by weight of water absorbed after soaking in water for 24 hours as shown in Equation (2). The M_a and M_s in Equation (2) represents the wet mass and dry mass of the sample, respectively. The porosity of the samples was also evaluated by using Equation (3) while Equation (4) was used to calculate the density. The P_o, A_w, and M_s in Equation (3) represents the porosity, water absorption coefficient and dry mass of the sample, respectively. M_ρ, M_s and V in Equation (4) represents the density, dry mass and apparent volume, respectively.

$$L = \frac{L_O - L_T}{L_O} \times 100 \tag{1}$$

$$WA = \frac{M_a - M_s}{M_s} \times 100 \tag{2}$$

$$P_o = \frac{A_w \times M_s}{100} \tag{3}$$

$$M_\rho = \frac{M_s}{V} \tag{4}$$

The strength properties of the clay composite were evaluated in terms of the flexural strength and compressive strength. The flexural strength (б) in expressed MPa was calculated for each specimen in accordance with ASTM F417 (1996) by using Equation (5). The F, L, b, and h in Equation (5) represents the force, span length and width of the samples, respectively. The compressive

strength (R_c) was evaluated using Equation (6), where F and S represent s the compressive load and cross-sectional area respectively. The sample size used for flexural strength is 40 mm × 40 mm × 160 mm while that use for compressive strength is 40 mm × 40 mm × 40 mm. Five samples were made for each sample group and the average results presented.

$$\sigma = \frac{3}{2}\frac{FL}{bh^2} \tag{5}$$

$$R_c = \frac{F}{S} \tag{6}$$

3. Results

3.1. Characterization of the Raw Clay Samples

3.1.1. Grain Size, Landing Limits and Geotechnical Classification

The results from the particle size analysis of the raw clays are presented in Table 1 and Figure 2. These findings showed that the Arg.Lat and Arg.All materials have 8% and 1% gravel and 60% and 41% sand respectively. The silty fraction is 7% (Arg.Lat) and 12% (Arg.All) while the clay fraction is 25% (Arg.Lat) and 46% (Arg.All), respectively. Arg.Lat is rich in clay and sand with the proportion of sand higher 60% against 25% clay while Arg.All is richer in clay 46% than sand 41%. Such differences in the weight content of the granulometric fractions certainly have an influence on the ceramic properties of these materials (shaping of the specimens, firing temperature, densification, etc.) and even on the mechanical properties of the compacted products. The lateritic clay has a yellowish-brown colour (7.5 YR 6/8) while the alluvial material has a light grey colour (7.5YR 7/2).

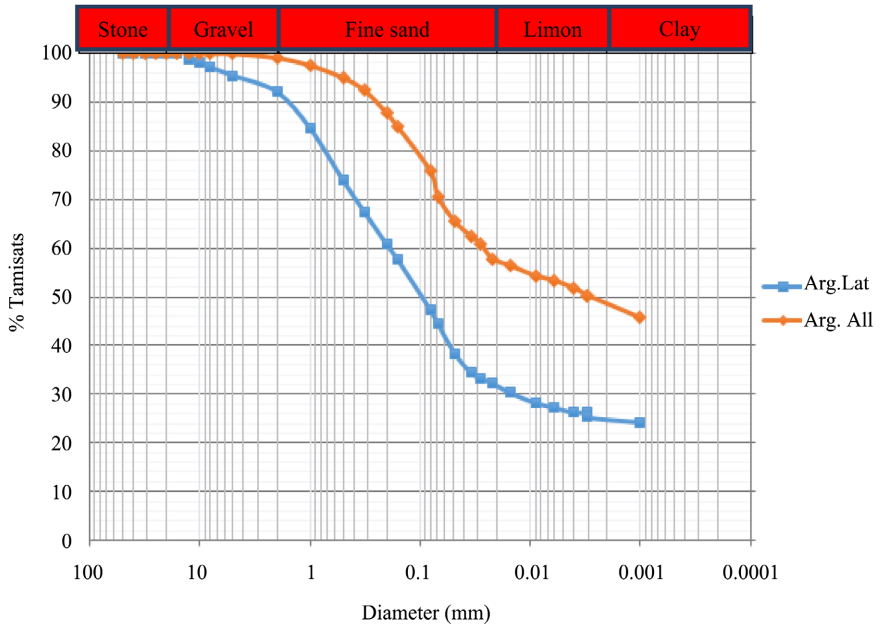

Figure 2. Particle size distribution of clay samples.

Table 1. Particle size analysis of the Batchenga clay materials.

Samples	Class	% of gravel $\Phi > 2$ mm	% of sand $2 > \Phi > 0.02$ mm	% of limons $0.02 > \Phi > 0.002$ mm	% of clay $\Phi < 0.002$ mm	Total
Arg.Lat	sandy	8	60	7	25	100
Arg.All	clayey	1	41	12	46	100

SHAPE * MERGEFORMAT.

The geotechnical properties of the clay samples are presented in **Table 2**. The values of the liquidity limits (WL) of the materials named Arg.Lat and Arg.All have distant average values and are 38.3% and 46.7% respectively. The plasticity limits (Wp) of Arg.Lat and Arg.All are 18.2% and 21.1% respectively while their plasticity indices are 20.3% (Arg.Lat) and 25.6% (Arg.All). It follows from these results that the lateritic clay sample (Arg.Lat) can take up about 38.3% water (ωL) and deform plastically with 18.2% water (ωp) on average. For the alluvial clay (Arg.All), it can take about 46.7% water (ωL) and deform plastically with 21.1% water (ωp) on average).

Figure 3 shows the position of these clay materials in the Casagrande plasticity chart. The fine fraction of the Arg.All sample is located in the domain of highly plastic silts and organic soils while the Arg.Lat sample is located in the domain of low plastic soils. The projection of these same results of granulometric analysis in the diagram of Winkler (1954) in Hajjaji *et al.* (2002) shows that these two clay samples fall in the domain required for building materials from the granulometric point of view as shown in **Figure 4**. The lateritic clay (Arg.Lat) corresponds to the production of dense bricks while the alluvial clay to bricks and masonry tiles.

The density values of the clay samples are respectively 15.13 kg/m^3 (Arg.Lat) and 14.39 kg/m^3 (Arg.All). This difference observed between the density values of these materials is due to the large amount of silicon oxide quantified by X-ray Fluorescence, which would make the latter denser, this observation confirms the work of Burrough [23]. The specific surface values are 28.63 m^2/g (Arg.Lat) and 118.18 m^2/g (Arg.All), respectively. The large value obtained from the alluvial clay (Arg.All) would be due to the presence of mineral phases such as illite, montmorillonite, the same observations were reported in [15].

3.1.2. Mineralogical and Chemical Composition

The diffractograms of Arg.Lat and Arg.All clays are shown in **Figure 5**. The Arg.Lat sample (**Figure 5(a)**) consists mostly of the crystalline phases such as quartz, kaolinite, hematite and calcite. The alluvial clay Arg.All (**Figure 5(b)**) is composed of quartz, kaolinite, hematite, calcite, corundum, gehlenite, montmorillonite, muscovite, albite, dolomite and halloysite. The chemical compositions of the clay samples are presented in **Table 3**. The majority oxides are 72.13 wt% SiO_2 (Arg.Lat), 48.91 wt% SiO_2 (Arg.All), 14.1 wt% Al_2O_3 (Arg.Lat), 23.79 wt% (Arg.All), 4.45 wt% Fe_2O_3 (Arg.Lat) and 9.53 wt% Fe_2O_3 (Arg.All). TiO_2 is

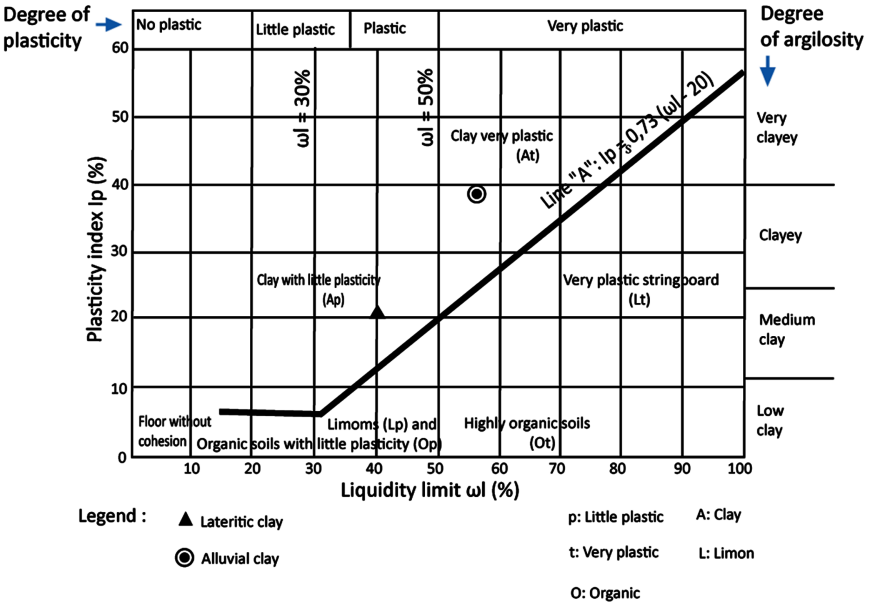

Figure 3. Position of Arg.Lat and Arg.All materials in the Casagrande plasticity chart.

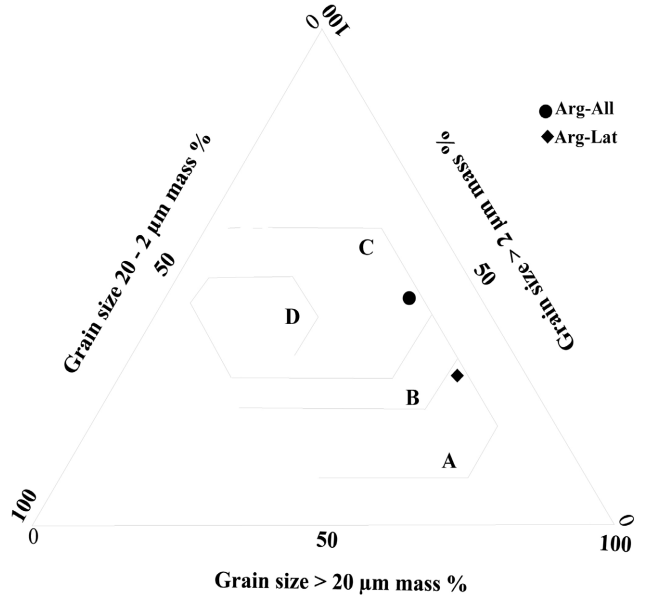

Figure 4. Position of Arg.Lat and Arg.All materials in the Winkler diagram in Hajjaji *et al.* (2002).

Table 2. Atterberg limits of the clay samples.

Samples	(ω_L) (%)	(ωp) (%)	(Ip) (%)	Apparent Density (kg/m^3)	Specific surface (m^2/g)
Arg.Lat	38.3	18.2	20.3	15.13	28.63
Arg.All	46.7	21.1	25.6	14.39	118.18

Table 3. Chemical composition (%).

	SiO_2	Al_2O_3	Fe_2O_3	TiO_2	K_2O	MgO	MnO	CaO	Na_2O	P_2O_5	SO_3	BaO	SrO	Cr_2O_3	PF 1000	Total
Arg.Lat	72.13	14.1	4.45	1.04	0.39	0.12	0.11	0.08	0.06	0.05	0.03	0.03	0.03	0.01	7.01	99.83
Arg.All	48.91	23.79	9.53	1.36	1.23	1.34	0.08	2.6	2.57	0.01	0.01	0.11	0.08	0.01	7.66	99.46

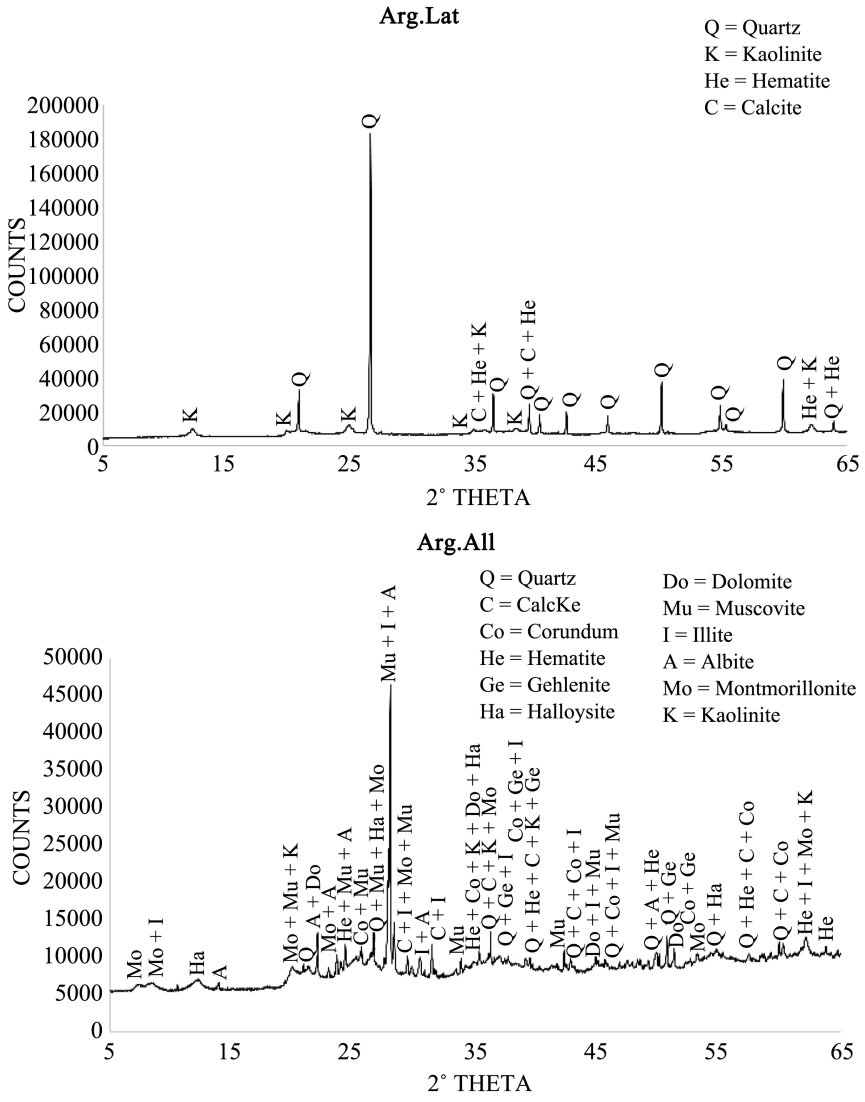

Figure 5. X-ray diffactogram of clay samples.

in low percentage in both clays 1.04% (Arg.Lat) and 1.36% (Arg.All). The contents 1.23% K_2O (Arg.All), 1.34% MgO (Arg.All), 2.6% CaO (Arg.All), and 2.57% Na_2O (Arg.All) are in low percentage in the alluvial clay and in trace amounts in the lateritic clay. P_2O_5 oxides, SO_3, BaO, SrO and Cr_2O_3 are also present in both clays in trace amounts. The presence of K_2O and MgO oxides in the alluvial clay confirms the presence of the illite and montmorillonite mineral phases detected on the X-ray diffractogram (**Figure 4(b)**), which would justify the large value of the specific surface obtained compared to the lateritic clay.

3.1.3. Thermogravimetric Analysis

The ATG/ATD thermograms of the materials Arg.All and Arg.Lat are shown in Figure 6. Between 0˚C and 100˚C, the ATG thermograms of the materials (Arg.All and Arg.Lat) indicate a small mass loss of less than 3% corresponding to the departure of the water of hydration [24]. Between 100˚C and 300˚C, an endothermic peak is observed on the ATD of the materials named Arg.All and Arg.Lat, so the optimum is reached 263˚C and 299˚C respectively. These endothermic peaks are accompanied by mass losses of 0.60% and 1.5% recorded on the ATG curves. These observed losses reflect the dehydroxylation of hydroxylated minerals such as goethite into hematite, which is expressed by the following equation.

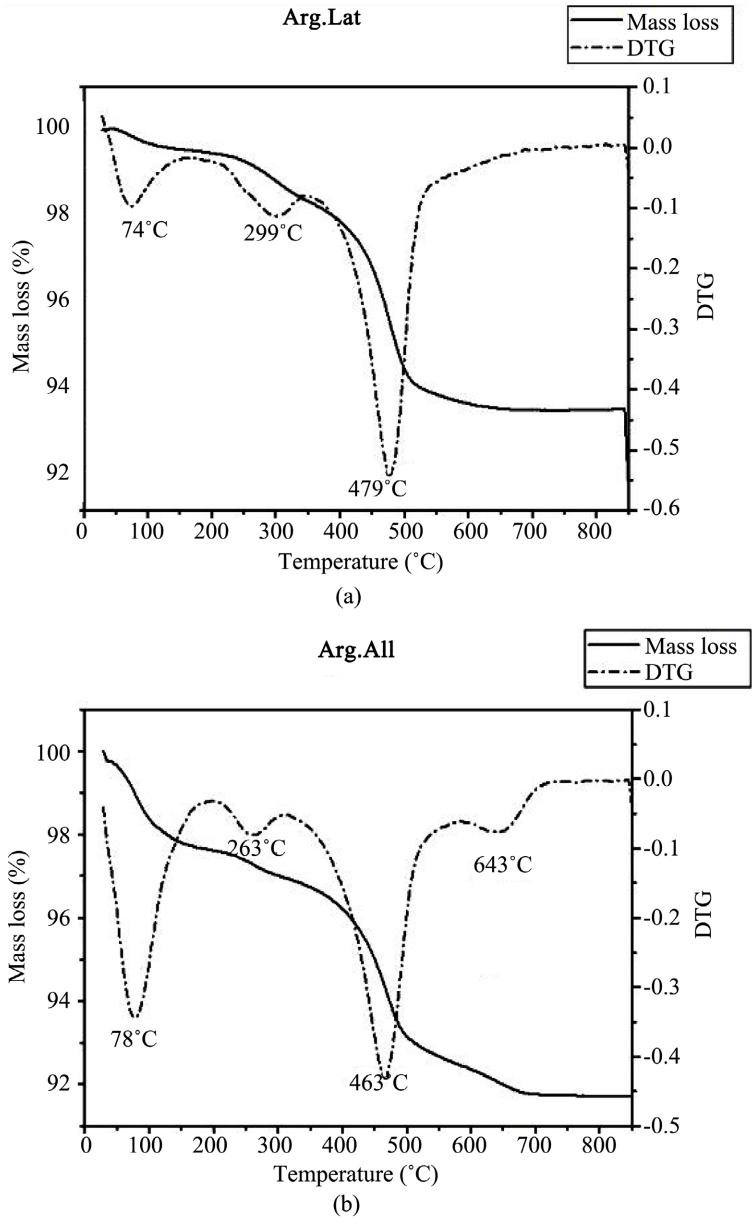

Figure 6. Thermographic ATG/ATD curves of clay samples.

$$2FeOOH \rightarrow Fe_2O_3 + H_2O \quad (6)$$

Between 300˚C and 500˚C, the ATD curves of the material (Arg.Lat and Arg.All) show optima at 463˚C and 479˚C respectively. These endothermic peaks are accompanied with the mass losses of 6.32%, 8.20% on the ATG curves. The mass losses observed on the Arg.Lat and Arg.All materials correspond to the dehyloxylation of the clay minerals kaolinite and halloysite leading to the formation of metakaolinite as depicted in Equation (7). The endothermic peak appearing at 643˚C, corresponds to the dehydroxylation of minerals such as muscovite and montmorillonite.

$$Si_2O_5Al_2(OH)_4 \rightarrow 2SiO_2 \cdot Al_2O_3 + 2H_2O \quad (7)$$

3.2. Properties of Fired Clay Composites

3.2.1. Appearance of the Composites

The Arg.All specimens show a dull brown colour at 900˚C and 1000˚C, which changes to a greyish colour at 1100˚C. The Arg.Lat samples change from yellowish brown to orange at the firing temperatures (900˚C, 1000˚C, 1100˚C). **Figure 7** shows the picture of the clay composites fired at different temperatures.

3.2.2. Linear Shrinkage

The evolution of linear shrinkage as a function of firing temperature is shown in **Figure 8**. It can be seen that in the 900˚C and 1000˚C range, the Arg.All and Arg.Lat samples show a linear shrinkage that increases from 5.76% to 8.56% and from 2.46% to 3.27% respectively. These values increase further to values of 13.21% and 3.75% respectively at 1100˚C. The linear shrinkage for any firing temperature is higher for the alluvial clay than for the lateritic clay. The low linear shrinkage observed on the clay composites is attributable to the low clay fraction content 25% compared to 46% (Arg.All). Thus, during firing, there would be less physico-chemical transformation in the lateritic clay compared to the alluvial clay.

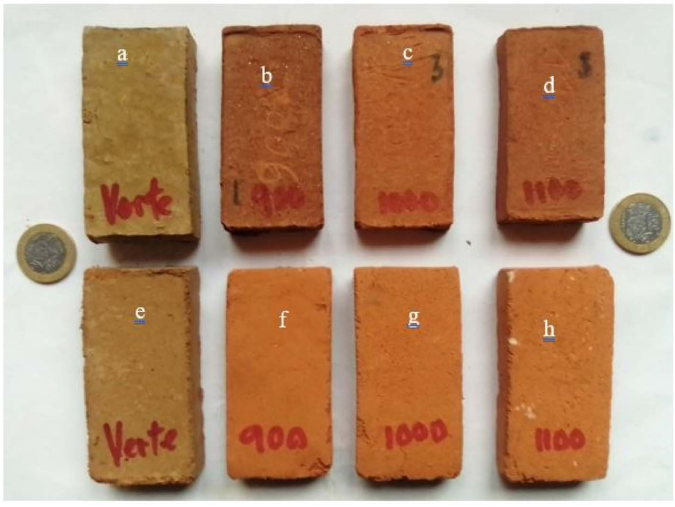

Figure 7. Arg.All composites ((a), (b), (c) and (d)), Arg.Lat ((e), (f), (g) and (h)).

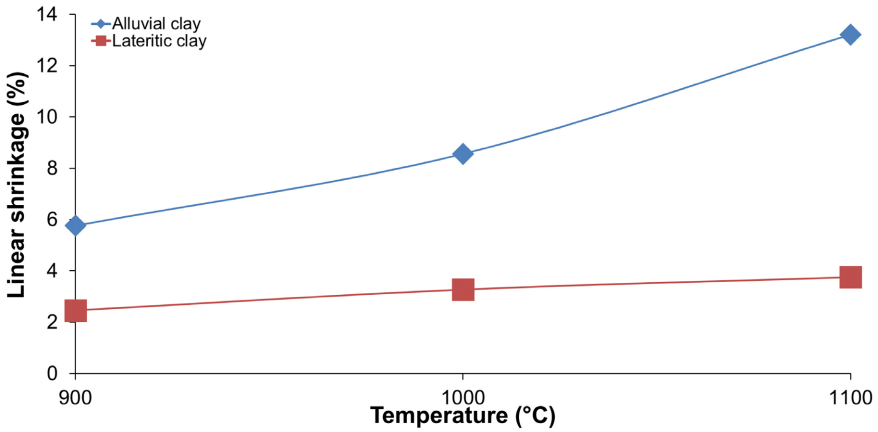

Figure 8. Variation of linear shrinkage as a function of firing temperature.

3.2.3. Mechanical Performance

The results of the mechanical properties of the clay composites in terms of the flexural strength and compressive strength are shown in **Figure 9**. In general, it is noted a significant increase in the mechanical measurements (bending and compression) with the increase of the firing temperature (900˚C to 1100˚C). The values of flexural strength are located between 0.53 and 0.76 MPa for clay composites obtained from (Arg.Lat) and between 4.45 and 6.8 MPa for those obtained from (Arg.All). The flexural strength values are very low for lateritic clays, less than 1 MPa for all temperatures. This low value of flexural strength is the result of the low percentage of the clay fraction in the Arg.Lat material which would ensure a good cohesion between the different particles. This trend is similar to the work of Ntouala *et al.* [25] and Bodian *et al.* Nyassa Ohandja *et al.* [26] who improved some mechanical properties of clay composites from lateritic clays by incorporating the clay materials at different percentage. Thus, the high percentage of the clay fraction in the Arg.All material justifies the high values of flexural strength obtained.

The values of compressive strengths are ranged between 5.36 and 6.88 MPa for Arg.Lat based clay composites and 17.50 and 27.38 MPa for those from Arg.All at temperatures 900˚C and 1100˚C respectively. They also increase as a function of the firing temperature. However, the compressive strength values of clay composites from Arg.Lat are for any firing temperature lower than those of clay composites from Arg.All at the same temperatures. According to these results, the alluvial clays offer better performances even at 900˚C (4.45 and 17.50 MPa, respectively for bending and compression) compared to the standards required according to the work of Souza *et al.* [27]. The hydroxylation of mineral phases such as illite, muscovite and montmorillonite contained in the alluvial clay would contribute to strengthen the matrix, which would justify the high mechanical performances. Increasing the firing temperature in the present study improved the mechanical properties as reported in [28] [29].

3.2.4. Water Absorption, Porosity and Density

Figure 10 shows the variation in the percentage of water absorbed from the

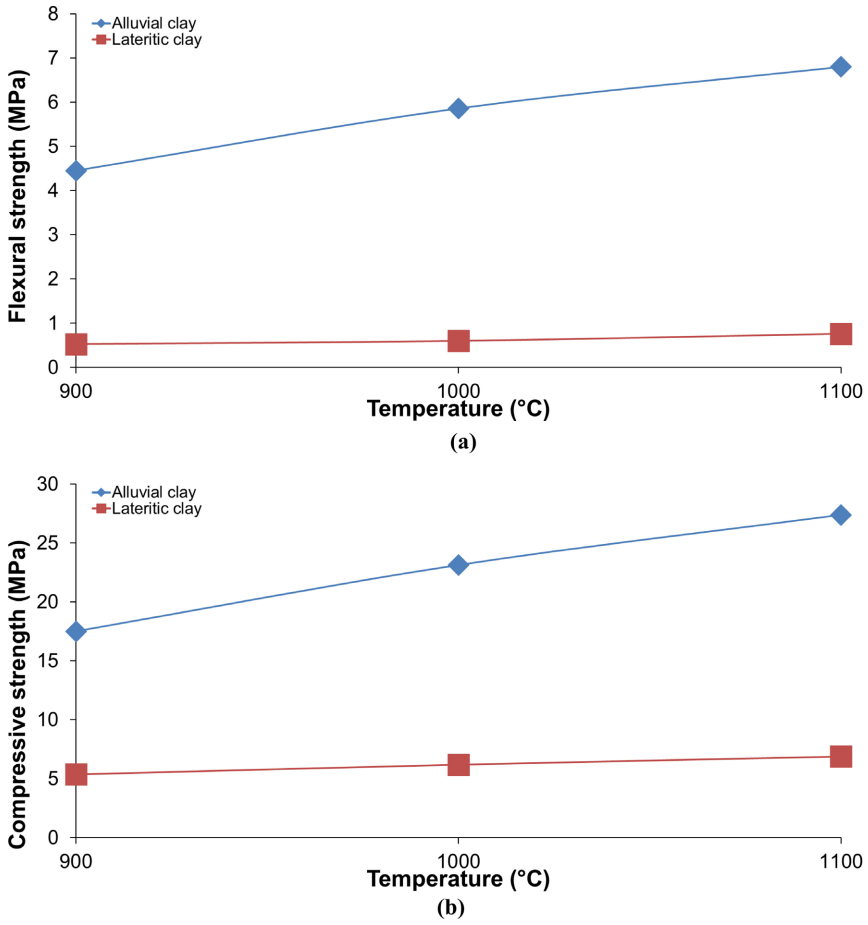

Figure 9. Mechanical peformance (a) flexural strength (b) compressive strength.

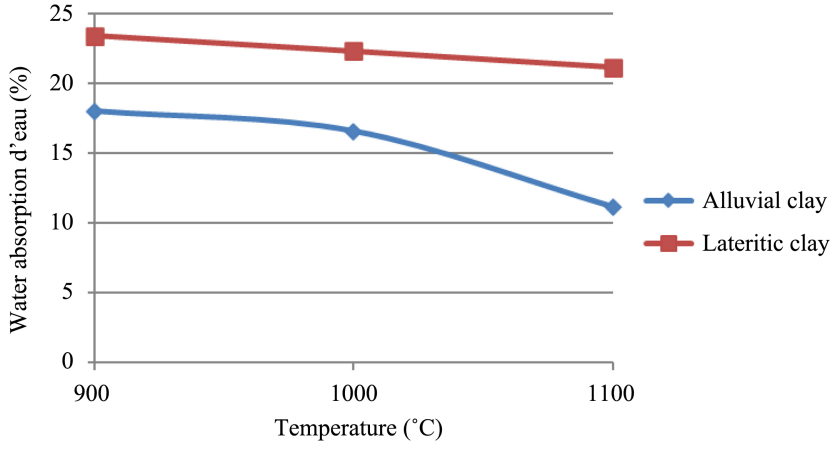

Figure 10. Water absorption of clay composites.

specimens as a function of the firing. It is evident that the water absorption decreases with higher firing temperature. The water absoprtion varies between 18% at 900˚C and 11.16% at 1100˚C for the alluvial clay sample (Arg.All) and between 23.43% and 21.16% respectively at the same temperatures for the lateritic clay sample (Arg.Lat). The lateritic clay-based samples show the highest water

absorption values. The low rate of water absorption of the clay composites from Arg.All is due to the presence of flux minerals (Albite, muscovite and gehlenite) which ensure a good cohesion between the different constituents and decrease the voids within the matrix. The presence of corundum also contributes to the densification of the matrix ensuring good mechanical properties as shown in Figure 9. Thus, once immersed in water for the test, these samples would fix less water compared to clay composites from Arg.Lat.

The same trend is observed with the porosity test (Figure 11) which decreases as the temperature increases. The porosity of the alluvial clay and lateritic clay blocks behave in the same way as the water absorption. The more voids a material has the more water it absorbs. The best result of porosity is revealed at 1100˚C, *i.e.* 22.93% for the alluvial clay and 36.01% for the lateritic clay at the same temperature.

The values of bulk density of the clay composites are presented in Figure 12. It can be seen that the density values increase from 900˚C to 1100˚C, *i.e.* 1.87 to 2.06 g/cm^3 for the alluvial clays. This trend is in agreement with the results of the mechanical resistances (Figure 7 and Figure 8). Thus, a high compactness induces a good densification, hence the high mechanical strength and the high

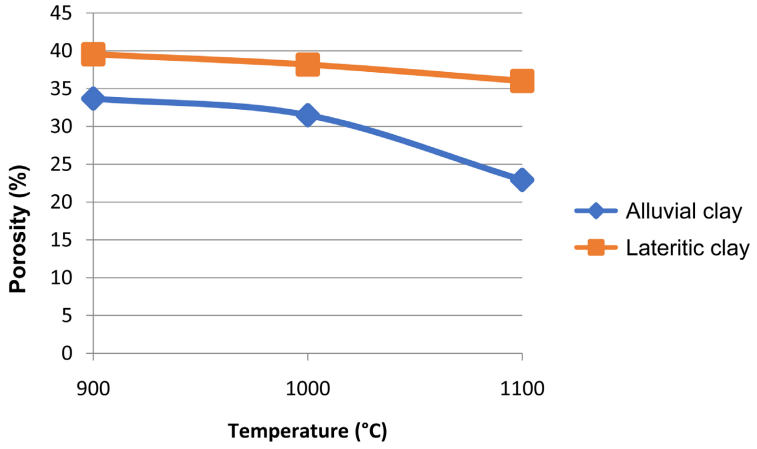

Figure 11. Porosity of clay composites.

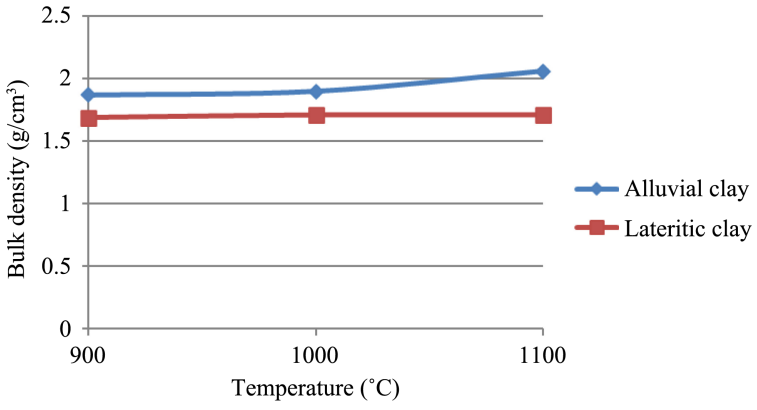

Figure 12. Density of clay composites.

density. For the clay composites from the lateritic clay Arg.Lat, these values are between 1.69 and 1.71 g/cm^3. These values increase by 0.2 g/cm^3 at 1000˚C and stabilize at 1100˚C or 1.71 g/cm^3 for lateritic clays. The small increase recorded here for these formulations would be due to the low cohesion and compactness between the different constituents within the matrix. This trend is in agreement with the results of porosity and water absorption. Thus, the presence of voids in the Arg.Lat clay composites would make them lighter unlike the products formed with Arg.All which are more compact and denser.

3.2.5. SEM Analysis

The selected micrographs of the clay composites Arg.All900 and Arg.Lat900 heated at 900˚C; Arg.Lat1100 and Arg.All1100 heat treated at 1100˚C describing their internal structure are shown in **Figure 13** and **Figure 14**. From this figure, it appears that the clay composite Arg.All100 presents a compact and dense structure compared to that of Arg.Lat1100. This observation is in agreement with the evolution of the results of the mechanical resistances. The densification of the microstructure of Arg.All100 is justified by the important clay fraction (46%) and the alkaline earths which, during the firing process, have largely contributed to a good cohesion between the different particles within the matrix, thus ensuring a high mechanical resistance.

On the other hand, the micrograph of Arg.Lat1100 highlights a less dense structure with voids, pores and microcracks along the matrix. The presence of these cracks, pores and non-homogeneity would be due to the low mechanical strength recorded on the Arg.Lat1100 sample. Thus, the presence of minerals such as MgO, K_2O and CaO by their high rate would justify the densification and compactness of the sample Arg.All1100 ensuring the best mechanical performance. The presence of pores and cracks observed on the Arg.Lat900 micrograph are at the origin of the high-water absorption and porosity rates. These voids, once the samples are immersed for 24 hours for the absorption test, retain a significant amount of water through the defects observed in the microstructure. The observed micrographs corroborate the mechanical and porosity results.

4. Discussion

The clays of Batchenga are composed of the following main minerals in decreasing order, SiO_2, Al_2O_3 and Fe_2O_3. These clays are siliceous materials. The mineralogical composition of the Batchenga alluvial clay is comparable to that obtained on the banks of the Sanaga River by Nzeukou *et al.* [30]. The Batchenga alluvial clay offers better clay composite compared to the lateritic clay based on their position in the Winkler (1954) diagram reported in **Figure 4**.

The water absorption values of Batchenga clays are higher than those obtained at Akok-Maka by Ntouala *et al.* [5] at the same temperatures. But at 1100˚C, the percentage of water absorbed from Arg.All is lower than that obtained by the same author at the same temperature. As a result, Arg.All would provide better firing products from the water absorption point of view. The samples based on

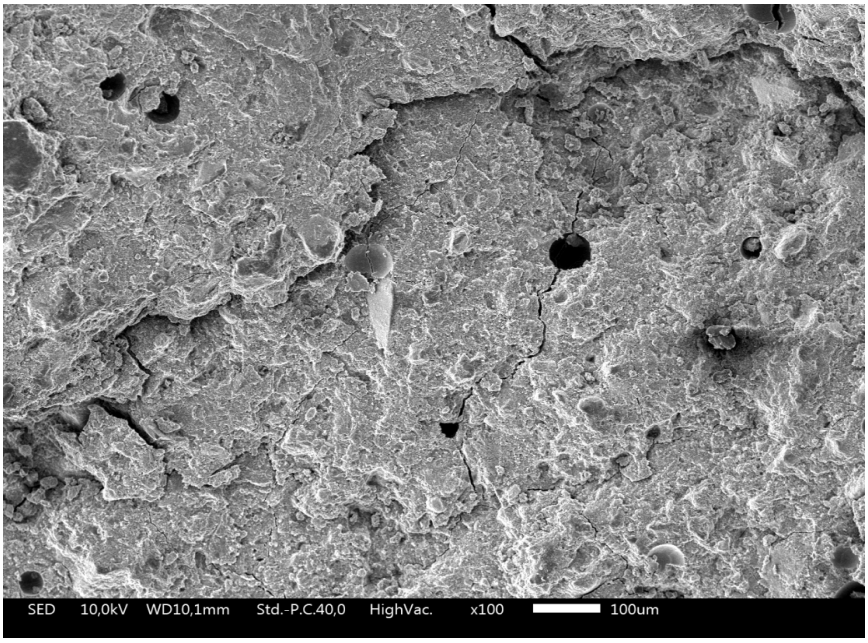

(a)

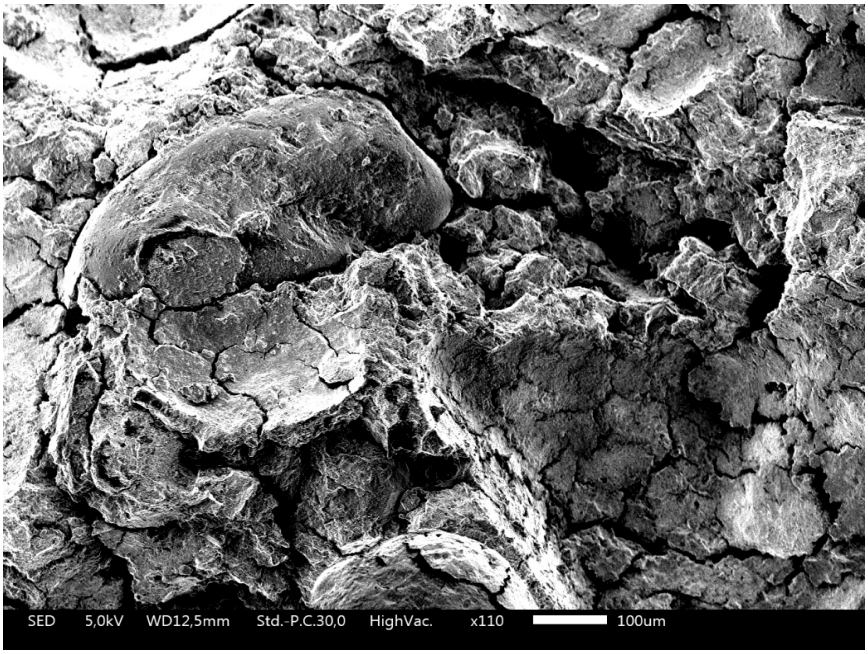

(b)

Figure 13. Microstructures of Arg.All (a) and Arg.Lat (b) products heated at 900˚C.

lateritic clay show the highest water absorption values. This is in agreement with the results obtained by Ntouala *et al.* [5] on lateritic and alluvial clays from Akok-maka. These results are comparable to those obtained at Ngaye by Djenabou *et al.* [13] on lateritic and alluvial clays at 900˚C and 1100˚C respectively. The (Aw) of the lateritic clay at Batchenga is higher than that at Ngaye while the water absorption values of the alluvial clays at Ngaye are all higher than that of Batchenga at 1100˚C.

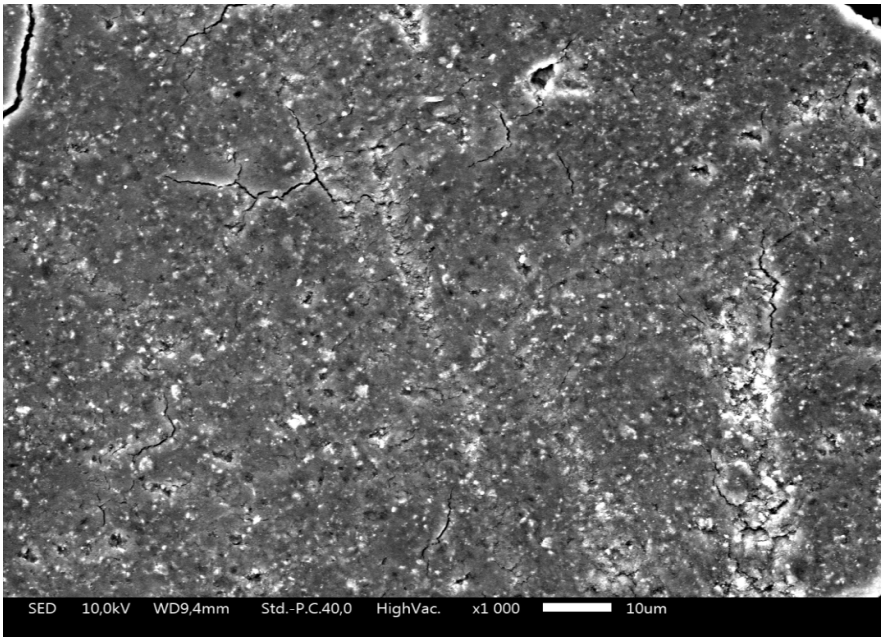

(a)

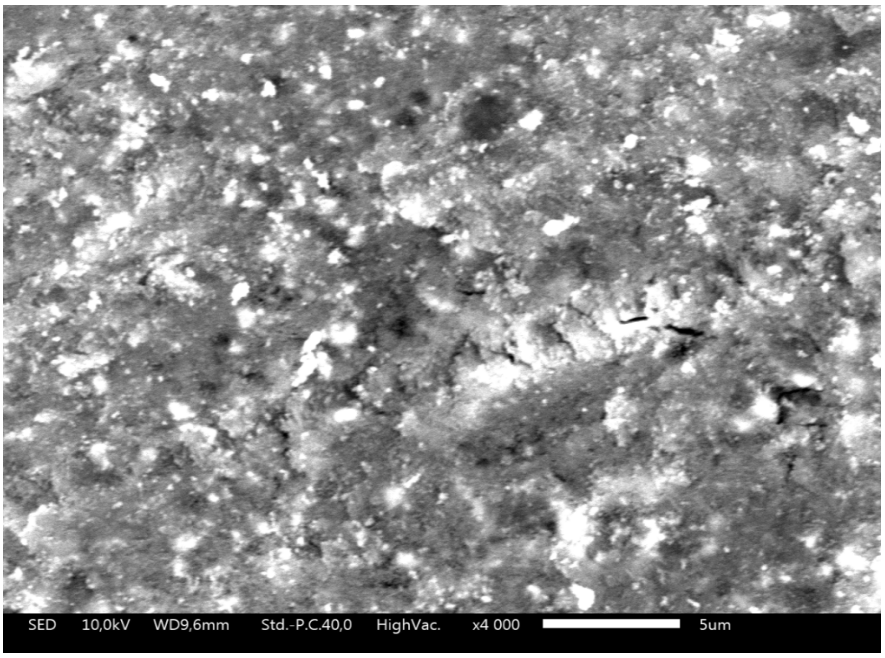

(b)

Figure 14. Microstructures of Arg.All heated at 1100˚C.

The mechanical strengths of the Batchenga clays needed improvement. The water absorption and flexural strength values specified by Souza *et al.* [27] are for dense bricks, Aw < 25% and Ϭ ≥ 2 Mpa; for clay composites and for roof tiles, Aw > 20% and Ϭ ≥ 6.5 Mpa. In comparison with the results obtained, all materials show water absorption rates < 25% and are therefore suitable for brick production from this point of view. From the flexural strength point of view, the lateritic clays (Arg.Lat) are unsuitable for the production of bricks for all tem-

peratures because of their flexural strength lower than 2 Mpa. Alluvial clay can be used for the production of dense bricks for all experimental temperatures. Concerning the production of roof tiles, the remaining water absorption of lateritic clay is higher than 20%, which is to be avoided, while that of alluvial clay is lower than 20% at all temperatures. From the point of view of flexural strength, except at 110˚C for alluvial clay (Arg.all) whose Ϭ is greater than 6.5 Mpa, all other Ϭ values are less than 6.5 Mpa. The Arg.All material, and this at 110˚C is suitable for tile production because of its high flexural strength.

5. Conclusion

The aim of this work was to valorize the firing products of two clays from the locality of Batchenga, one lateritic (Arg.Lat) and the other alluvial (Arg.All), with a view to their use in the construction of decent and low-cost housing for the local population. Arg.Lat and Arg.All have 20.3% and 25.6% plasticity index and are classified as low plasticity sandy-clay and high plasticity sandy-clay soils respectively. Their chemical compositions contain silica, alumina and iron. Alkalis (K_2O) and alkaline earths (CaO, MgO) are more important (7.74%) in Arg.All, low in Arg.Lat (0.5%). In addition to quartz, kaolinite, hematite and calcite found in both clays, Arg.All also contains feldspars, corundum, montmorillonite, dolomite and illite. The compressive and flexural mechanical parameters increase with firing temperature and are higher in Arg.All than in Arg.Lat for all experimental temperatures. At 100˚C, their values in compression are 27.38 MPa (Arg.All) and 6.88 MPa (Arg.Lat) and in flexure they are 6.80 MPa (Arg.All) < 1 Mpa (Arg.Lat). Because of its flexural strength < 2 MPa, Arg.Lat is unsuitable for the production of bricks for all firing temperatures. However, Arg.All is suitable for the production of ceramic products and even roof tiles at 100˚C because the flexural strength exceeds 6.5 MPa. Furthermore, its industrial potential is estimated at 2.2 10^5 tones with the most suitable geotechnical performance.

Acknowledgements

The authors recognize the assistance of the staff of the Laboratory at the MIPROMALO for their assistance in the characterization of raw materials and end products.

Conflicts of Interest

The authors declare no conflicts of interest regarding the publication of this paper.

References

[1] Millot, G.J.P. (1964) Géologie des Argiles. Masson et Cie, Echandens, 499.

[2] Taallah, B., Guettala, A., Guettala, S. and Kriker, A. (2014) Mechanical Properties and Hygroscopicity Behavior of Compressed Earth Block Filled by Date Palm Fibers. *Construction and Building Materials*, **59**, 161-168. https://doi.org/10.1016/j.conbuildmat.2014.02.058

[3] Mimboe, A.G., Abo, M.T., Djobo, J.N.Y., Tome, S., Kaze, R.C. and Deutou, J.G.N. (2020) Lateritic Soil Based-Compressed Earth Bricks Stabilized with Phosphate Binder. *Journal of Building Engineering*, **31**, Article ID: 101465. https://doi.org/10.1016/j.jobe.2020.101465

[4] Ngon, N. (2007) Etude morphologique, minéralogique, géochimique et cristallographique des argiles latéritiques et des argiles hydromorphes de la région de Yaoundé en zone tropicale humide. Essais industriel et evaluation de leurs potentialités comme matériaux de construction. Université de Yaoundé I, Cameroun.

[5] Ntouala, R. (2014) Produits d'altération des schistes et argiles alluviales de la série d'Ayos à Akok-Maka (Est-Cameroun): Minéralogie, géochimie et valorisation agro-pédologique et géotechnique. Thèse Doctorat Ph-D, Faculté des Sciences, Université de Yaoundé I, Cameroun.

[6] Mbumbia, L., Mertens de Wilmars, A. and Tirlocq, J. (2000) Performance Characteristics of Lateritic Soil Bricks Fired at Low Temperatures: A Case Study of Cameroon. *Construction and Building Materials*, **14**, 121-131. https://doi.org/10.1016/S0950-0618(00)00024-6

[7] Ngon, G.F.N., Etame, J., Ntamak-Nida, M.J., Mbog, M.B., Mpondo, A.M.M., Gérard, M., Yongue-Fouateu, R. and Bilong, P. (2012) Geological Study of Sedimentary Clayey Materials of the Bomkoul Area in the Douala Region (Douala Sub-Basin, Cameroon) for the Ceramic Industry. *Comptes Rendus Geoscience*, **344**, 366-376. https://doi.org/10.1016/j.crte.2012.05.004

[8] Thibault, P. and Le Berre, P. (1985) Les argiles pour brique. Vol. 65, Bureau de Recherches Géologiques et Minières, Orléans.

[9] Kamseu, E., Kaze, C.R., Fekoua, J.N.N., Melo, U.C., Rossignol, S. and Leonelli, C. (2020) Ferrisilicates Formation during the Geopolymerization of Natural Fe-Rich Aluminosilicate Precursors. *Materials Chemistry and Physics*, **240**, Article ID: 122062. https://doi.org/10.1016/j.matchemphys.2019.122062

[10] Kaze, C.R., Nana, A., Lecomte-Nana, G.L., Deutou, J.G.N., Kamseu, E., Melo, U.C., Andreola, F. and Leonelli, C. (2022) Thermal Behaviour and Microstructural Evolution of Metakaolin and Meta-Halloysite-Based Geopolymer Binders: A Comparative Study. *Journal of Thermal Analysis and Calorimetry*, **147**, 2055-2071. https://doi.org/10.1007/s10973-021-10555-2

[11] Kaze, R.C., Beleuk à Moungam, L.M., Fonkwe Djouka, M.L., Nana, A., Kamseu, E., Chinje Melo, U.F. and Leonelli, C. (2017) The corrosion of Kaolinite by Iron Minerals and the Effects on Geopolymerization. *Applied Clay Science*, **138**, 48-62. https://doi.org/10.1016/j.clay.2016.12.040

[12] Mbey, J.A. (2013) Films composites amidon de manioc-kaolinite: influence de la dispersion de l'argile et des interactions argile-amidon sur les propriétés des films. Université de Lorraine, Lorraine.

[13] Fadil-Djenabou, S., Ndjigui, P.-D. and Mbey, J.A. (2015) Mineralogical and Physicochemical Characterization of Ngaye Alluvial Clays (Northern Cameroon) and Assessment of Its Suitability in Ceramic Production. *Journal of Asian Ceramic Societies*, **3**, 50-58. https://doi.org/10.1016/j.jascer.2014.10.008

[14] Youmoue, M., Fongang, R.T.T., Sofack, J.C., Kamseu, E., Melo, U.C., Tonle, I.K., Leonelli, C. and Rossignol, S. (2017) Design of Ceramic Filters Using Clay/Sawdust Composites: Effect of Pore Network on the Hydraulic Permeability. *Ceramics International*, **43**, 4496-4507. https://doi.org/10.1016/j.ceramint.2016.12.101

[15] Nzeugang Nzeukou, A., Fagel, N., Njoya, A., Beyala, Kamgang, V., Eko Medjo, R., and Chinje Melo, U. (2013) Mineralogy and Physico-Chemical Properties of Alluvi-

al Clays from Sanaga Valley (Center, Cameroon): Suitability for Ceramic Application. *Applied Clay Science*, **83**-**84**, 238-243.
https://doi.org/10.1016/j.clay.2013.08.038

[16] Nzeukou Nzeugang, A., Medjo Eko, R., Fagel, N., Kamgang Kabeyene, V., Njoya, A., Balo Madi, A., Mache, J.R. and Melo Chinje, U. (2013) Characterization of Clay Deposits of Nanga-Eboko (Central Cameroon): Suitability for the Production of Building Materials. *Clay Minerals*, **48**, 655-662.
https://doi.org/10.1180/claymin.2013.048.4.18

[17] Deutou, N.J.G., Beda, T., Biesuz, M., Boubakar, L., Melo, U.C., Kamseu, E. and Sglavo, V.M. (2018) Design and Characterization of Porous Mullite Based Semi-Vitrified Ceramics. *Ceramics International*, **44**, 7939-7948.
https://doi.org/10.1016/j.ceramint.2018.01.232

[18] Deutou, J.N.G., Kamga, V.E.L.S., Kaze, R.C., Kamseu, E. and Sglavo, V.M. (2020) Thermal Behaviour and Phases Evolution during the Sintering of Porous Inorganic Membranes. *Journal of the European Ceramic Society*, **40**, 2151-2162.
https://doi.org/10.1016/j.jeurceramsoc.2020.01.035

[19] Deutou, J.N.G., Zounedou, N., Kaze, R.C., Mohamed, H., Beda, T., Melo, U.C., Kamseu, E. and Sglavo, V.M. (2019) Semi-Vitrified Porous Kyanite Mullite Ceramics: Young Modulus, Microstructure and Pore Size Evolution. *SN Applied Sciences*, **2**, Article No. 126. https://doi.org/10.1007/s42452-019-1902-5

[20] Ekodeck, G.E. (1984) L'altération des roches métamorphiques du Sud Cameroun et ses aspects géotechniques. Doctral Thesis, Scientific and Medical University of Grenoble, Grenoble.

[21] Vallerie, M. (1995) La pédologie: Planche 2. In: *Atlas régional Sud-Cameroun*, Office de la recherche scientifique et technique outre-mer, Yaoundé, 6-7.

[22] Nzenti, J.P., Barbey, P., Macaudiere, J. and Soba, D. (1988) Origin and Evolution of the Late Precambrian High-Grade Yaounde Gneisses (Cameroon). *Precambrian Research*, **38**, 91-109. https://doi.org/10.1016/0301-9268(88)90086-1

[23] Burrough, P.A. (2001) Fractals in Soil Science. *European Journal of Soil Science*, **52**, 527-528. https://doi.org/10.1046/j.1365-2389.2001.00418-10.x

[24] Kakali, G., Perraki, T., Tsivilis, S. and Badogiannis, E. (2001) Thermal Treatment of Kaolin: The Effect of Mineralogy on the Pozzolanic Activity. *Applied Clay Science*, **20**, 73-80. https://doi.org/10.1016/S0169-1317(01)00040-0

[25] Ntouala, R.F.D., Onana, V.L., Kamgang, V. and Ekodeck, G.E. (2016) Mineralogical, Geochemical and Mechanical Characterization of the Ayos (East-Cameroon) Lateritic and Alluvial Clayey Mixtures: Suitability for Building Application. *Journal of Building Engineering*, **5**, 50-56. https://doi.org/10.1016/j.jobe.2015.11.007

[26] Nyassa Ohandja, H., Ntouala, R.F.D., Onana, V.L., Ngo'o Ze, A., Ndzié Mvindi, A.T. and Ekodeck, G.E. (2020) Mineralogy, Geochemistry and Physico-Mechanical Characterization of Clay Mixtures from Sa'a (Center Cameroon): Possibly Use as Construction Materials. *SN Applied Sciences*, **2**, 1687.
https://doi.org/10.1007/s42452-020-03365-y

[27] Souza, G., Sánchez, R. and De Holanda, J.J.C. (2002) Characteristics and Physical-Mechanical Properties of Fired Kaolinitic Materials. *Ceramica*, **48**, 102-107.
https://doi.org/10.1590/S0366-69132002000200009

[28] Diao, I., Diagne, M. and Dia, I. (2021) Applications, Characterization of Fired Clay Bricks for an Economic Contribution of the Exploitation of Thicky Clay Deposit. *Materials Sciences and Applications*, **12**, 389-416.
https://doi.org/10.4236/msa.2021.129027

[29] Voula, R.M., Diamouangana, F.Z.M., Moutou, J.-M., Samba, V.I.B., Foutou, M.P. and Ngoma, M. (2021) Characterization, and Engineering, Characterization and Valuation of a Clay Soil Sampled in Londéla-Kayes in the Republic of Congo. *Journal of Minerals and Materials Characterization and Engineering*, **9**, 117-133. https://doi.org/10.4236/jmmce.2021.92009

[30] Nzeukou, N.A., Traina, K., Medjo, E.R., Kamseu, E., Njoya, A., Melo, U.C., Kamgang, B.V., Cloots, R. and Fagel, N. (2014) Mineralogical and Physical Changes during Sintering of Plastic Red Clays from Sanaga Swampy Valley, Cameroon. *Interceram - International Ceramic Review*, **63**, 186-192. https://doi.org/10.1007/BF03401056